Pete Gagnon[1]
Chia-Wei Cheung[2]
Paul J. Yazaki[2]

[1]Validated Biosystems, San Clemente, CA, USA
[2]Division of Cancer Immunotherapeutics and Tumor Immunology, Beckman Research Institute, City of Hope, Duarte, CA USA

Received January 28, 2009
Revised June 29, 2009
Accepted September 2, 2009

Research Article

Cooperative multimodal retention of IgG, fragments, and aggregates on hydroxyapatite

Retention mapping of chimeric monoclonal IgG_1, Fc, Fab, $F(ab')_2$, and aggregated antibody was conducted on hydroxyapatite (HA) by systematically varying phosphate and chloride concentrations during gradient elution in order to characterize the interactions of each solute with calcium and phosphate residues on the solid phase. Lysozyme was used as a control to model cation exchange-dominant interactions. Bovine serum albumin was used as a control for calcium affinity-dominant interactions. Calcium affinity and phosphoryl cation exchange were positively cooperative for IgG-related species. Fc retention was dominated by calcium affinity, while retention of Fab was dominated by cation exchange. $F(ab')_2$ exhibited a curve shape similar to Fab, but stronger retention. The retention curve for intact IgG incorporated the distinctive elements of its fragments but stronger retention than that predicted by their addition to one another. Aggregate retention paralleled the curve for non-aggregated antibody, with stronger retention by both binding mechanisms. Experimental data revealed evidence of charge repulsion between IgG carboxyls and HA phosphate at low conductivity values. Electrostatic repulsion of amino residues and attraction of carboxyls by HA calcium appeared to be blocked by strong complexation of calcium with mobile phase phosphate.

Keywords: Binding mechanisms / Hydroxyapatite / IgG aggregates / IgG fragments
DOI 10.1002/jssc.200900055

1 Introduction

Hydroxyapatite (HA) has demonstrated valuable utility in the field of IgG purification for its ability to remove aggregates [1–6], to achieve single-step IgG purity approaching levels achieved by affinity methods [7, 8], and to purify Fab and other fragmentary constructs [9–12]. In addition to the economic value of these applications, the well-characterized structures of IgG and related entities make them suitable probes to investigate the surface reactivity of HA. The above studies, reporting on about 20 IgG monoclonal antibodies, have demonstrated that IgG is retained dominantly by a combination of calcium metal affinity and phosphoryl cation exchange, regardless of subclass, light chain type, or p*I*. These studies have also contributed important refinements to our understanding of IgG interactions with HA. For example, although total phosphate concentration correlates well with antibody retention, dibasic phosphate ions are the primary eluents, while the effects of monobasic phosphate are relatively minor [6]. Zeta-potential measurements have revealed that charge shielding by different buffering species and eluents also plays a significant role in net selectivity [6]. Glycosylation does not significantly affect retention of IgG [6, 9]. Antibody retention generally becomes weaker with increasing pH [6, 9], as does retention of most proteins [13].

A number of interactions predicted by studies on peptide and protein models remain uncharacterized. Crystal surface calcium atoms each bear a single positive charge, potentially capable of mediating electrostatic interactions with protein residues, including attraction of carboxyls and repulsion of amino residues [14–19]. HA phosphates may repel protein carboxyls, in addition to their documented ability to bind amino groups. Dissecting the individual influence of these potential interactions is complicated by the arrangement of calcium and phosphate on the crystal surface. Surface calcium atoms are surrounded by an inner perimeter of three negatively charged oxygen atoms, about 120 pm distant, and an outer perimeter of three more at about twice that distance (Fig. 1) [15, 16]. This close proximity of HA calcium and phosphate groups highlights the potential for cooperativity among HA interactions. This further complicates interpretation by creating nonlinear adsorption isotherms that defy models based on simpler

Correspondence: Pete Gagnon, Validated Biosystems, 240 Avenida Vista Montana, Suite 7F, San Clemente, CA 92672, USA
E-mail: pete_gagnon@mac.com
Fax: +1-949-606-1904

Abbreviations: CV, column volume; **HA,** hydroxyapatite; **MVM,** minute virus of mice; **MuLV,** murine leukemia virus

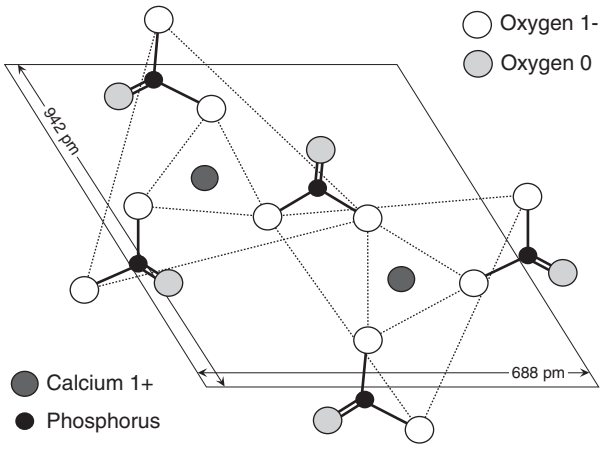

Figure 1. Distribution of charges on the crystal surface of HA. The parallelogram represents a portion of the crystal surface perpendicular to its longitudinal axis. The small triangles mark the inner perimeter of negatively charged oxygen molecules surrounding each surface calcium atom. The larger triangles mark the outer perimeter. Note that each unit shares an oxygen atom from the neighboring unit so that while each calcium is surrounded by six negatively charged oxygen atoms, the net ratio in the frame of the illustration is actually 5:1. Refer to Sections 1, 3.1, and 3.2 for discussion. The figure is modified from the one in [11]. Refer to the original reference for additional information and citations describing crystal structure.

adsorption mechanisms [20]. Cooperativity is described as positive in cases where multimodal interactions produce progressively stronger binding and negative where interactions depress net retention.

The most revealing mechanistic studies of IgG retention to date have employed combinations of phosphate and sodium chloride [3, 6]. Phosphate elutes both primary retention mechanism; its high calcium affinity competes with calcium affinity interactions between HA and proteins; its conductivity weakens ion exchange interactions. Chloride acts primarily on ion exchange interactions; it has little effect on calcium affinity. The inherent limitation of these studies is that they have mostly been conducted for the purpose of aggregate removal, and the ranges of the key variables have been limited to practical operating ranges for HA. In the present study, we evaluate more extensive grids of phosphate gradients at different sodium chloride concentrations, and sodium chloride gradients at different phosphate concentrations in the hope of refining the model of IgG retention on HA. Practical applications of the data to process development and validation are discussed.

2 Materials and methods

2.1 Materials and equipment

Rituxan® (rituximab, Genentech, South San Francisco, CA, USA), a chimeric IgG_1 anti-CD20 monoclonal antibody, was used to produce Fab, $F(ab')_2$, and Fc fragments. Immobilized papain and pepsin was obtained from Thermo Fisher Scientific, Rockford, IL, USA. A monoclonal antibody containing about 40% aggregates was a generous gift from Avid BioServices, Tustin, CA, USA. Lysozyme, BSA, and buffer components were purchased from Sigma/Aldrich, St. Louis, MO, USA. Ceramic hydroxyapatite CHT™ Type I, 40 μm, was obtained from Bio-Rad Laboratories, Hercules, CA, USA and packed into 1 mL (5 × 50 mm) MediaScout® columns by ATOLL GmbH, Weingarten, Germany. CIM® SO_3 cation-exchange and QA anion-exchange monoliths (334 μL, 16 × 3 mm) were obtained from BIA Separations, Klagenfurt, Austria. All chromatography experiments were performed on an AKTA® Explorer 100, GE Healthcare, Piscataway, NJ, USA.

2.2 Experimental procedures

2.2.1 Preparation of antibody fragments and aggregates

Purified Rituxan was digested with immobilized papain or pepsin following the manufacturer's instructions. Briefly, the antibody and immobilized enzyme gel were equilibrated to the specified buffer. About 100 mg of antibody was added to 5 mL of immobilized enzyme gel slurry and incubated at 37°C for 16 h with end-to-end mixing. The immobilized enzyme was removed by centrifugation. The digested preparation was dialyzed into 25 mM Tris, 50 mM sodium chloride pH 7.5, sterile filtered, and stored at −20°C. Antibody fragments were purified by HA chromatography with a linear gradient from 5–200 mM sodium phosphate, pH 7.0. Purified aggregates were prepared from the high-aggregate antibody by HA chromatography with a sodium chloride gradient conducted at 10 mM sodium phosphate, pH 7.0, as described in [4]. Aggregates were dominantly composed of four IgG molecules [4].

2.2.2 Chromatography on HA

A series of experiments to evaluate the combined effects of phosphate and calcium was conducted by running sodium chloride gradients over a range of phosphate concentrations. The HA column was equilibrated with 20 mM Hepes, pH 7.0, at a linear flow rate of 600 cm/h (2 mL/min). An aliquot of 100 μL of sample was injected, and the column washed with equilibration buffer. The sample was eluted with a 20 column volume (CV) linear gradient to 20 mM Hepes, 1.0 M sodium chloride, pH 7.0. The column was cleaned with 500 mM sodium phosphate, pH 7.0. In the next experiment, the equilibration, wash, and elution buffers contained 5 mM sodium phosphate. In subsequent experiments, both buffers contained 10, 20, 40, 80, or 160 mM sodium phosphate. A corresponding series was conducted at pH 8.5, substituting 20 mM Tris for Hepes.

Another series was developed by conducting phosphate gradients at different chloride concentrations. The column was equilibrated with 20 mM Hepes, pH 7.0, loaded,

washed, and eluted with a 20 CV linear gradient to 160 mM sodium phosphate, pH 7.0. It was then cleaned with 500 mM sodium phosphate, pH 7.0. A second experiment was run with 10 mM sodium chloride in both gradient buffers. Subsequent runs were conducted in the presence of 20, 40, 80, and 160 mM sodium chloride. Between experimental series, the column was stored in 20% ethanol, 10 mM sodium phosphate, pH 7.0.

It is important to note that the conditions under which many of the above experiments were conducted may damage HA. The distributor recommends that HA not be operated in the absence of 5 mM phosphate [21].

2.2.3 Ion exchange chromatography

Cation and anion exchange monoliths were equilibrated with 20 mM Hepes, pH 7.0, at a volumetric flow rate of 4 mL/min. About 100 µL of Fab, $F(ab')_2$, Fc, or intact Rituxan were injected, and the columns washed with equilibration buffer. The samples were eluted with a 60 CV (20 mL, 5 min) linear gradient to 20 mM Hepes, 1.0 M sodium chloride, pH 7.0.

2.2.4 Isoelectric focusing

p*I* determinations for Rituxan, $F(ab')_2$, Fab, and Fc were performed with a Novex IEF pH 3–10 gel system (Invitrogen, Carlsbad, CA, USA) and compared with IEF protein standards (Serva Electrophoresis, Heidelberg, Germany).

3 Results and discussion

3.1 Retention of IgG

Figure 2 plots retention of Rituxan in sodium chloride gradients at different phosphate concentrations (pH 7.0). Retention was plotted against conductivity instead of sodium chloride concentration to capture the conductivity contribution of phosphate. Corresponding sodium chloride concentrations are presented in Table 1. Retentions of lysozyme and BSA are plotted in the same figure to represent the behavior of cation exchange-dominated and calcium affinity-dominated proteins. BSA (p*I* ~4.7) is dominated by calcium affinity. It failed to elute in sodium chloride gradients at phosphate concentrations up to 40 mM phosphate but failed to bind at 60 mM phosphate (Fig. 2). Its steep response curve resembles the early part of the IgG curve. The 40 mM horizontal offset in phosphate concentration between the curves indicates that IgG has much lower calcium affinity than BSA. This is consistent with Rituxan's p*I* of 9.5–10, suggesting a relative deficiency of carboxyl groups. This would also be understood to limit the number of polycarboxyl domains configured appropriately to support coordination with HA calcium. Lysozyme (p*I* ~11) is dominated by cation exchange. It elutes in a sodium chloride gradient even in the absence of phosphate, and

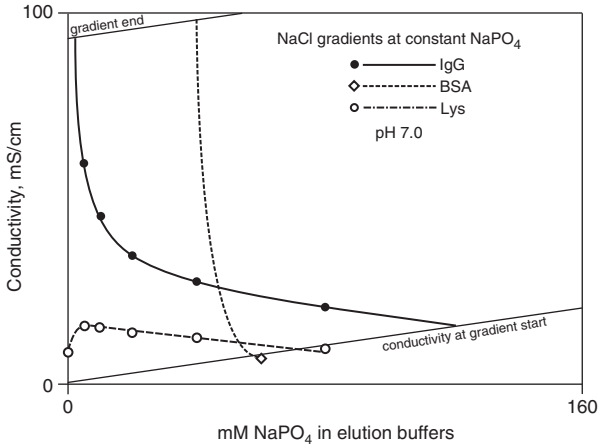

Figure 2. Retention of IgG, BSA, and Lysozyme (Lys) as a function of conductivity in sodium chloride gradients at various phosphate concentrations (pH 7.0). Data points below the line of conductivity at gradient start indicate that the solute was unretained under the specified conditions. Elution chloride concentration and conductivity values are presented in Table 1. Refer to Section 2.2.2 for more detailed discussion of experimental conditions and to Sections 3.1 and 3.2 for discussion of the data.

exhibits a shallow linear decline in retention as phosphate is added to the elution buffers. It resembles the latter portion of the IgG retention curve, except that retention of IgG is much stronger. Rituxan's p*I* is slightly lower than lysozyme. This suggests that its stronger cation exchange binding reflects a larger number of interactions, consistent with the more than tenfold greater mass of IgG, but it could also indicate a cooperative contribution by calcium affinity.

Figure 3 plots retention of Rituxan, BSA, and lysozyme *versus* conductivity in phosphate gradients at different sodium chloride concentrations (pH 7.0). Corresponding phosphate concentrations are presented in Table 2. The figure exhibits the distinctive contributions of calcium affinity and cation exchange binding in a very different context, and reveals other influences. The most striking feature of the figure is that elution conductivities ascend with increasing sodium chloride concentration. This is unheard of with ion exchangers and highlights the conductivity resistance of calcium affinity, as exemplified by BSA. At sodium chloride concentrations greater than 10 mM, the BSA curve ascends nearly parallel with the line created by the conductivity at gradient start for the various experiments. This demonstrates virtual immunity to sodium chloride, which in turn indicates the weak contribution of electrostatic interactions.

The lysozyme curve in Fig. 3 ascends at a much shallower angle than BSA and rapidly converges with the gradient start line. That it ascends at all illustrates a positive contribution by calcium affinity. If binding were exclusively electrostatic, the curve would be horizontal. Calcium affinity is weak, however, as illustrated by non-retention at 160 mM sodium chloride. Convergence of the lysozyme curve with the line marking conductivity at gradient start signifies loss

Table 1. Elution sodium chloride concentration and conductivity at peak center in sodium chloride gradients run at indicated phosphate concentrations (pH 7.0)[a)]

Solute	Phosphate concentration and conductivity increment during chloride gradient					
	0/0.6	5/1.3	10/2.0	20/3.2	40/5.9	80/10.4
	Sodium chloride concentration (mM) and conductivity (mS/cm) at peak center					
IgG	NE	634/60.1	501/48.3	331/33.3	248/27.8	160/21.4
$F(ab')_2$	NE	381/37.1	335/32.3	291/28.6	222/24.7	136/20.25
Fab	550/53.6	266/25.4	235/22.9	200/20.2	148/17.2	NR
Fc	NE	407/39.4	373/36.4	107/11.0	NR	NT
Mab2	NE	584/55.9	429/41.8	343/34.26	285/30.0	163/23.0
Aggr.	NE	967/88.8	685/64.8	495/48.3	371/38.4	251/31.1
Lys	137/8.6	258/15.6	245/15.3	218/11.13	125/10.5	NR
BSA	NE	NE	NE	NE	NR	NT

a) NE indicates that the solute failed to elute within the gradient. NR indicates that it was not retained. NT indicates that it was not tested.

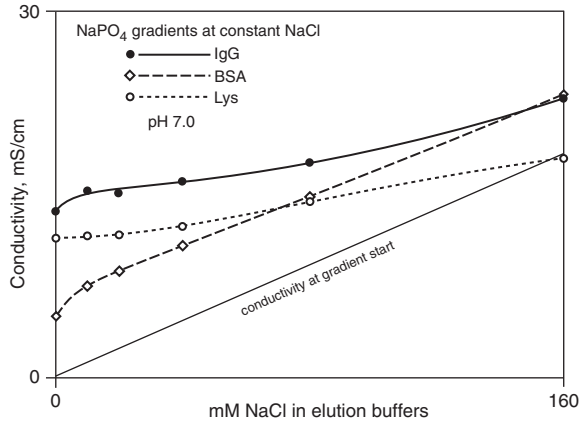

Figure 3. Retention of IgG, Lysozyme, and BSA as a function of conductivity in sodium phosphate gradients at various sodium chloride concentrations (pH 7.0). Data points below the line marking conductivity at gradient start indicate that the solute was not retained under the specified conditions. Eluting phosphate concentration and conductivity values for the above solutes plus Fc and Fab are presented in Table 2. Refer to Section 2.2.2 for more detailed discussion of experimental conditions and to Sections 3.1 and 3.2 for discussion of the data.

of electrostatic binding with increasing chloride concentration. This is understood to represent cation exchange between HA phosphate and lysozyme amino residues. The slope of the IgG curve is essentially parallel with lysozyme at 80 mM sodium chloride, possibly reflecting its similar p*I*. The IgG slope diverged from lysozyme at 160 mM sodium chloride, becoming more positive, conforming more closely to the line marking conductivity at gradient start, and thereby revealing its stronger calcium affinity.

The BSA and IgG curves in Fig. 3 exhibit depressed retention in the absence of sodium chloride. A similar phenomenon was observed for lysozyme in the absence of phosphate (Fig. 2). These features suggest the influence of interactions that weaken retention. Previous work has shown that DNA elutes from HA at about 225 mM phosphate in a phosphate gradient absent sodium chloride, but elutes at about 460 mM phosphate in the presence of 1.0 M sodium chloride [22]. Weaker retention absent sodium chloride was attributed to restricted contact of DNA phosphates with HA calcium due to electrostatic repulsion between HA phosphates and DNA phosphates. Sodium chloride was believed to suppress this effect, allowing DNA to participate in more coordination events with HA calcium. BSA is far less charged than DNA but still heavily carboxylated, suggesting that its retention might also be depressed to some degree by repulsion from HA phosphates. The present data suggest that negative charge repulsion of BSA is indeed comparatively slight, since its effects are apparent only at conductivity values below about 7.5 mS/cm. This suggests in turn that the majority of BSA carboxyls are involved in coordination interactions with HA calcium. The parallel low conductivity response of Rituxan equally suggests the effects of charge repulsion, but this conclusion is challenged by its low carboxylation relative to BSA. This could be the explanation, nevertheless. Early work with HA emphasized that single carboxyls were not able to participate in calcium affinity interactions [17–19]. If the number of IgG carboxyls not involved in calcium affinity interactions were roughly similar to BSA, negative charge repulsion at low conductivity should also be similar.

Rituxan's high p*I* raises the possibility that the lower retention absent NaCl might reflect charge repulsion between HA calcium and IgG amino residues, but this is challenged by the behavior of lysozyme. First, lysozyme's retention in Fig. 3 does not exhibit the low conductivity depression manifested by IgG. Second, lysozyme's behavior in Fig. 2 points to a specific mechanism by which all kinds of electrostatic interactions with HA calcium might be eliminated. Soluble calcium forms such a strong association with HA phosphate that it completely suspends phosphoryl cation exchange [12, 17–19, 23]. The association is stable even in the presence of 1.0 M sodium chloride [12]. We

Table 2. Elution phosphate concentration and conductivity at peak center in sodium phosphate gradients run at the indicated sodium chloride concentrations (pH 7.0)[a)]

Solute	Chloride concentration and conductivity increment during phosphate gradient					
	0/0.6	10/1.7	20/3.0	40/5.4	80/9.8	160/18.9
	Sodium phosphate concentration (mM) and conductivity (mS/cm) at peak center					
IgG	105/13.9	115/15.4	106/15.2	92/16.1	70.2/17.7	46.6/22.9
Fab	78/10.8	76/11.0	72/11.3	60/12.1	33/13.5	8.6/20.2
Fc	41/5.9	43/6.8	40/7.2	31/8.6	16/11.4	NR
Lys	85/11.4	81/11.6	71/11.7	61//12.4	42/14.3	NR
BSA	40/5.0	53/7.6	49/8.5	45/10.8	47/14.8	52/23.1

a) NR indicates that the solute was not retained under the specified conditions.

suggest that similarly strong pairing between HA calcium and mobile phase phosphate ions eliminates electrostatic interactions involving HA calcium. Figure 2 suggests that 5 mM phosphate is sufficient to suspend electrostatic repulsion of lysozyme. If sufficient for lysozyme, it should be sufficient for IgG. Lysozyme fails to show the effect in Fig. 3 because it elutes far above that threshold, at about 85 mM phosphate (Table 2). Note that this hypothesis also predicts that HA calcium should be incapable of electrostatically binding protein carboxyl residues in the presence of greater than 5 mM phosphate. Thus, it appears, in the presence of phosphate, that HA calcium is able to participate solely in coordination interactions.

Ion exchange chromatography results were consistent with the above data and interpretations. Rituxan failed to bind to the anion exchanger at pH 7, which would have been predicted by its alkaline p*I*. It bound strongly to the cation exchanger at the same pH and eluted at 11.3 mS (135 mM sodium chloride). It bound to an HA column equilibrated at 10.4 mS (80 mM phosphate, Table 1), but failed to bind HA at 160 mM phosphate. This demonstrates reasonable conformance of cation exchange binding with HA when calcium affinity was quenched by phosphate. A similar result was reported for another IgG_1 by Schubert and Freitag [9].

Overall, these data portray IgG retention on HA as embodying cation exchange retention roughly equivalent with dedicated cation exchangers, weak calcium affinity, very weak electrostatic repulsion between HA phosphate and IgG carboxyls, and no electrostatic interactions with HA calcium (in the presence of phosphate). Positive cooperativity between cation exchange and calcium affinity dominates retention. This interpretation, especially concerning cooperativity, is also consistent with published retention data in the form of dynamic binding capacity values. A mouse monoclonal IgG with a capacity of only 5 mg/mL in 500 mM sodium chloride absent phosphate, and only 11 mg/mL at 8 mM phosphate absent sodium chloride, bound with a dynamic capacity of 43 mg/mL in the absence of both [5]. Similar behavior of other monoclonal IgGs in sodium chloride gradients conducted at low phosphate concentrations [3, 5, 6, 24], and early observations of altered retention by polyclonal IgG upon inclusion of sodium chloride in phosphate gradients [25] suggest that this model should be broadly applicable, but individual variation may be considerable. A recent study of 15 different IgG monoclonals showed that the relative contributions of calcium affinity and phosphoryl cation exchange each varied by a factor of 2 [6].

3.2 Retention of fragments and aggregates

Retention curves for Rituxan Fab, $F(ab')_2$, and Fc (pH 7.0) in sodium chloride gradients at different phosphate concentrations also demonstrate cooperative binding, but each fragment exhibits distinctive contributions by calcium affinity and cation exchange (Fig. 4). Refer to Table 1 for sodium chloride concentration data. Fab was the only IgG derivative to elute in a sodium chloride gradient absent phosphate, eluting at 53.6 mS. Retention dropped by more than half to 25.4 mS at 5 mM phosphate, but dropped only about 25%, from 22.9 to 17.2 mS, over the range of 10–40 mM phosphate. These data indicate much weaker calcium affinity than intact IgG, but comparison with retention on the cation exchanger demonstrates that cooperative enhancement by calcium affinity is still substantial. Fab eluted from the cation exchanger at 6.2 mS/cm, less than 12% of the conductivity at which it eluted from HA absent phosphate. Even at 40 mM phosphate, sufficient calcium affinity remained to boost retention nearly threefold over the cation exchanger, to 17.2 mS. From 10 to 80 mM phosphate, the Fab retention curve essentially overlapped with the lysozyme curve (compare with Fig. 2), illustrating Fab's dominant retention by cation exchange. The p*I* of Rituxan Fab was about 10, and its mass is only about 33% of intact IgG, both of which would be expected to reduce its retention compared with intact IgG, as shown. These observations are supported by the behavior of Fab in phosphate gradients at different chloride concentrations (Table 2, Fig. 5). The early part of the Fab curve overlaps with lysozyme (Fig. 3), illustrating cation exchange retention. With increasing sodium chloride concentrations, the curve becomes more parallel with the

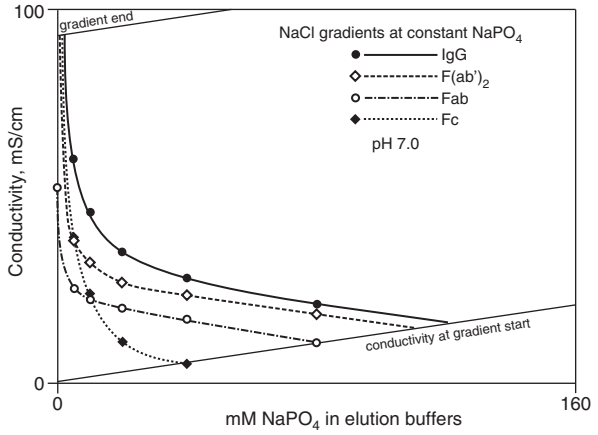

Figure 4. Retention of IgG, $F(ab')_2$, Fab, and Fc as a function of conductivity in sodium chloride gradients at various phosphate concentrations (pH 7.0). Data points intersecting the line marking conductivity at gradient start indicate that the solute was retarded but not retained under those conditions. Elution chloride concentration and conductivity values are presented in Table 1. Refer to Section 2.2.2 for more detailed discussion of experimental conditions and to Section 3 for discussion of the data.

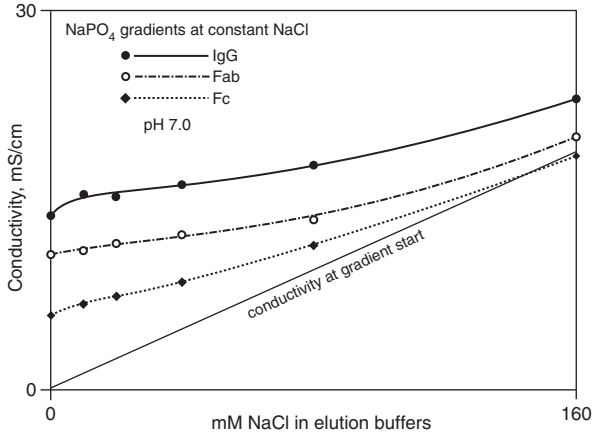

Figure 5. Retention of IgG, Fab, and Fc as a function of conductivity in sodium phosphate gradients at various sodium chloride concentrations (pH 7.0). Data points below the line marking conductivity at gradient start indicate that the solute was not retained under the specified conditions. Eluting phosphate concentration and conductivity values are presented in Table 2. Refer to Section 2.2.2 for more detailed discussion of experimental conditions and to Sections 3.1 and 3.2 for discussion of the data.

line indicating conductivity at gradient start. This illustrates progressive loss of cation exchange binding while revealing a persistent contribution by calcium affinity.

$F(ab')_2$ retention differed from Fab in two respects, the first of which was stronger binding by cation exchange. This was expected for two reasons: The p*I* of $F(ab')_2$ was greater than 10, as indicated by its failure to enter the IEF gel. Its larger size should also correspond to at least twice the number of binding interactions. The failure of $F(ab')_2$ to elute in a sodium chloride gradient absent phosphate also suggests stronger calcium affinity than Fab, but the increment might be smaller than implied since cooperative enhancement by stronger cation exchange binding could also be significant.

Absent phosphate, Fc failed to elute from HA at 1.0 M sodium chloride (~93 mS/cm), in spite of eluting at only 8 mS from the cation exchanger (Fig. 4). Its p*I* of 7.3 suggests proportionately higher carboxyl content than either $F(ab')_2$ or Fab, which in turn suggests that it failed to elute because of calcium affinity. The curve shape of Fc was similar to BSA, with both dropping from no elution to no retention over a span of about 20 mM phosphate (compare Figs. 2 and 4). This shows that calcium affinity is the dominant retention mechanism for Rituxan Fc. The steeper slope of the Fc curve compared with IgG, and stronger binding than Fab in the absence of phosphate, suggest that Fc calcium affinity is intermediate between the two. Phosphoryl cation exchange for Fc was the weakest of all fragments: it failed to bind HA at 40 mM phosphate (5.9 mS). Data from phosphate gradients at different salt gradients support identical conclusions (Fig. 5). Weaker Fc retention at all conductivities illustrates lower cation exchange binding, and the closer conformance of the slope with the line indicating conductivity at gradient start illustrates the relative dominance of calcium affinity.

Sodium chloride gradients at different phosphate concentrations at pH 8.5 paint a similar picture to chloride gradients at pH 7.0, but with dramatically weaker retention (Table 3, Fig. 6). Retention was reduced by roughly half for IgG, $F(ab')_2$, and Fab, but by about eightfold for Fc. It makes sense that the cation exchange component of binding should be reduced since proteins generally become less electropositive with increasing pH. The change in the titration state of phosphate ions would also increase their ion exchange elution potential since their molar conductivity increases about 20% from pH 7.0 to 8.5 (compare conductivity increments in Tables 1 and 3). The larger relative reduction for Fc retention could be an indication that it contains a higher proportion of histidyl residues than other solutes, which would be expected to lose positive charge at pH 8.5. This suggestion is consistent with its p*I* and the evolutionary conservation of a histidyl triplet in the hydrophobic cleft between the Cγ1 and Cγ2 domains on each side of the molecule [26–29]. It is likely that reduced Fc retention also reflects the weakening of HA calcium affinity that occurs with increasing pH [9, 13]. This would be expected to disproportionately reduce retention of solutes dominated by calcium affinity.

Compound IgG-related structures exhibit the distinctive retention features of their components but bind more strongly. All examples suggest cooperativity, but most manifest too many confounding influences to express it with precision. Tetra-aggregates bound more strongly than IgG, by both calcium affinity and cation exchange, but not by a factor of 4 (Fig. 7). This makes sense since associations among the individual IgG components must inevitably

Table 3. Elution sodium chloride concentration and conductivity at peak center in sodium chloride gradients run at indicated phosphate concentrations (pH 8.5)[a)]

Solute	Phosphate concentration (mM) during chloride gradient					
	0/0.8	5/1.9	10/2.8	20/4.4	40/7.2	80/12.4
Solute	Sodium chloride concentration (mM) and conductivity (mS/cm) at peak center					
IgG	NE	423/36.1	364/28.6	284/24.1	177/15.7	NR
$F(ab')_2$	NE	330/27.9	285/23.8	237/19.7	206/16.1	NR
Fab	632/55.6	264/20.6	246/17.3	173/14.1	NR	NT
Fc	NE	NR	NT	NT	NT	NT

a) NE indicates that the solute failed to elute within the gradient. NR indicates that it was not retained. NT indicates that it was not tested.

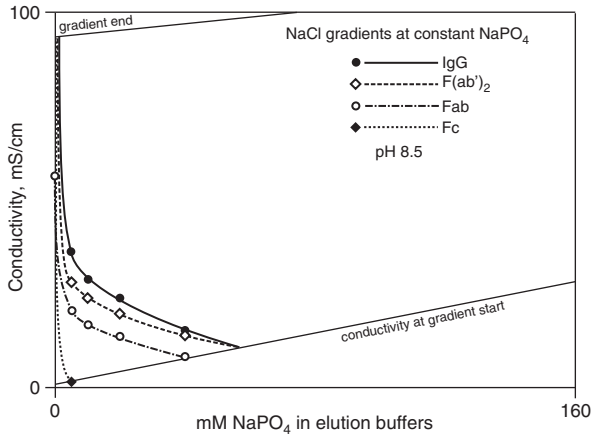

Figure 6. Retention of IgG, $F(ab')_2$, Fab, and Fc as a function of conductivity in sodium chloride gradients at various phosphate concentrations (pH 8.5). Data points intersecting the line marking conductivity at gradient start indicate that the solute was retarded but not retained under those conditions. Sodium chloride concentration and conductivity values are presented in Table 3. Refer to Section 2.2.2 for more detailed discussion of experimental conditions and to Section 3.2 for discussion of the data.

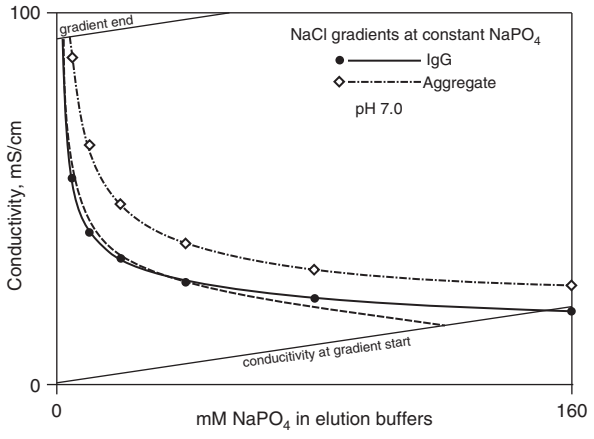

Figure 7. Retention of IgG and aggregates as a function of conductivity in sodium chloride gradients at various phosphate concentrations (pH 7.0). The antibody was unretained at 160 mM phosphate. Aggregates eluted at 160 mM phosphate in 216 mM sodium chloride, and conductivity of 26.8 mS/cm. Aggregates were unretained at 320 mM phosphate. All other values are presented in Table 1. The lighter weight dashed line reproduces the curve for Rituxan from Fig. 2 for comparison. Refer to Section 2.2.2 for more detailed discussion of experimental conditions and to Sections 3.2 and 3.3 for discussion of the data.

block some interactions with HA. This fits the definition for negative cooperativity. Retention of $F(ab')_2$ is similarly less than twice the retention of Fab (Fig. 4). This is a more complex situation since their charge characteristics are distinct, but it could illustrate negative cooperativity arising from conformational restrictions imposed by the linkage. Numerous studies have shown that proteins orient themselves preferentially so as to bind by the surface with the highest degree of complementarity to the solid phase [9, 30–34].

The incorporation by the IgG curve of the distinctive curve shapes of its fragments is one of the most compelling findings of the entire study; it dramatically manifests the distinctive retention characteristics of both Fc and $F(ab')_2$ (Fig. 4). It was more strongly retained than suggested by addition of Fc and $F(ab')_2$ retention. This could be an example of positive cooperativity, but for this to be the case would require that the conformational constraints imposed on the Fab and Fc regions of the integrated molecule increase the number of binding interactions, which is the opposite of what was observed with Fab and $F(ab')_2$. The p*I*s of IgG and its fragments provide no insight into the probability of either scenario.

It is noted throughout the above discussion that various aspects of IgG and fragment retention are consistent with their p*I*s within an experimental series. This is not to suggest that p*I* is predictive of HA retention as a general matter. p*I* correlates poorly with HA retention for the majority proteins [13], including antibodies [6, 9]. Even within the present study, the elution order of Fab and Fc was reversed in sodium chloride gradients at 0–10 mM phosphate *versus* 20 mM and higher (Fig. 4). This highlights the contribution of calcium affinity and the hazards of making broad conclusions about the effects of p*I* on selectivity of HA [3, 6, 9]. Additional contributions by charge repulsion, and the dominant expression of cation exchange

groups on the surface of HA can only be expected to further confound the correlation.

3.3 Practical applications

The phosphate-chloride gradients employed in the present study represent an extension of an approach that has proven useful for discovering the most effective conditions for removing aggregates from a given monoclonal IgG preparation [3]. The greater the vertical offset between the elution conductivities for aggregated and non-aggregated antibody at a given phosphate concentration, the greater the separation. Figure 7 thus recommends that a sodium chloride gradient be applied at 5 mM phosphate. We evaluated aggregate separation in phosphate gradients at different salt concentrations but observed no separation under any conditions. This result is consistent with other publications and presentations indicating that sodium chloride gradients at constant low phosphate concentrations tend to support the most effective aggregate removal for IgGs [2–6, 35–37]. Aggregates can be separated in simple phosphate gradients for some IgG antibodies, and bear worthy practical advantages [5, 37]. All buffers can be made as dilutions of the 500 mM phosphate-cleaning buffer, and the elution conductivity of the antibody is usually low enough to support application to an ion exchanger with little more than moderate pH titration and dilution. The high conductivities at which antibodies elute in chloride gradients requires that the HA step be placed at the end of the purification process, or that the eluate be buffer exchanged to permit compatibility with a subsequent ion exchange step.

The phosphate-chloride grid approach may also be applied in purification process development for fragmentary constructs. As an example from Fig. 4, Fab and Fc co-elute in a sodium chloride gradient at 10 mM phosphate, but are well separated in a chloride gradient at 20 mM phosphate where Fc fails to bind. This approach may also be useful in the purification of recombinant constructs from cell culture media, where BSA is a frequent contaminant. Since BSA requires 40–60 mM phosphate to elute, sodium chloride gradients at lesser phosphate concentrations will elute the product selectively, leaving BSA bound to the column. More than 3 logs of DNA, more than 4 logs of endotoxin, 3–4 logs of MuLV, and about 2 logs of MVM are also removed by this approach [3, 5, 38]. Phosphate gradients are also useful for purification of Fab, minibodies, and diabodies [10, 11]. In the event that BSA co-elutes with a given product in a phosphate gradient absent sodium chloride, addition of chloride will cause the construct to elute earlier while leaving BSA retention essentially unaltered (Table 2).

For any application, the phosphate-chloride grid approach provides a systematic characterization tool that can be used to support process validation. With sodium chloride gradients for example, the variation in the vertical offset between two contaminants over a specified range of phosphate concentration illustrates the sensitivity of the separation to variations within that range. Grid results can thus be used to document the quantitative response of the process to any pertinent variable, and to document that process specifications lie within a range where routine variations in such variables will not adversely affect process control.

The question naturally arises of how the grid approach compares with robotic high-throughput screening systems, such as described in [6]. Both approaches represent a rational data-driven approach to process design and validation, and both should lead to the same conclusions. Robotic systems produce more data points *per* unit time, but with substantial overhead costs. The grid approach can be employed at lower cost and offers the advantage of being able to model flow rate-dependent variables such as capacity and resolution. Statistical design of experiments can be used to reduce the number of experiments for either approach, but results from the present study reveal an important caution: the effects of phosphate concentration are not linear over a broad range. A preliminary series of experiments should therefore be conducted to identify a narrow range of interest, within which design of experiments may be applied confidently.

4 Concluding remarks

Results from this and other recent studies recommend several refinements to retention models that have been previously suggested for IgG. Some studies have suggested that HA calcium affinity is unaffected by conductivity [3, 4, 24]. This is imprecise. Even lysozyme has some calcium affinity (Fig. 3), and it elutes in a chloride gradient absent phosphate (Fig. 2), as does at least one monoclonal IgG [9]. This documents that very weak calcium affinity interactions can be eluted exclusively by increasing conductivity, and suggests that stronger calcium affinity interactions are probably affected to some degree. Electrostatic repulsion between IgG carboxyls and HA phosphate occurs simultaneously with the dominant interactions of calcium affinity and phosphoryl cation exchange, but appears to be damped out at low conductivities and probably has a negligible effect on selectivity under typical elution conditions. All electrostatic interactions between protein charged residues and HA calcium are probably blocked by its strong complexation with mobile phase phosphate.

While this model provides new insights concerning the interaction of IgG with HA, it remains far from complete and far from predictive. Many elements of HA interactivity with proteins remain inadequately characterized. The potential for HA to form hydrogen bonds with proteins has been known for decades [17–19] but its quantitative contribution remains undefined. Calcium affinity also requires more extensive characterization. Initial studies indicate that HA calcium lacks significant affinity for histidine clusters on IgG [24] and that calcium affinity is mediated, at least

partly, through protein carboxy clusters [17–19, 39]. Whether amino groups are also involved, including those in the peptide backbone, as in interactions between calcium and EDTA or EGTA, also remains to be determined. Crystallography studies have revealed that surface calcium atoms express only a single positive charge [15, 16], which raises the implication that the number of potential coordination sites is also reduced, and suggests in turn that its interactions with proteins may differ from soluble calcium. Hopefully, the substantial and growing economic importance of therapeutic antibodies, combined with the compelling abilities of HA for their purification, will encourage investigators to address these and other remaining questions.

Some parts of this research were supported by NCI grant CA43904.

The authors have declared no conflict of interest.

5 References

[1] Josics, D. J., Loster, K., Kuhl, R., Noll, F., Reusch, J., *Biol. Chem. Hoppe-Seyler* 1991, *372*, 149–156.

[2] Guerrier, L., Flayeux, I, Boschetti, E., *J. Chromatogr. B* 2001, *755*, 37–46.

[3] Gagnon, P., Ng, P., Aberin, C., Zhen, J., He, J., Mekosh, H., Cummings, L., Richieri, R., Zaidi, S., *BioProcess Intnl.* 2006, *4*, 50–60.

[4] Gagnon, P., *J. Immunol. Met.* 2008, *336*, 222–228.

[5] Gagnon, P., Beam, K., *Curr. Pharm. Biotechnol.* 2009, *25*, 287–293.

[6] Wensel, D., Kelley, B., Coffman, J., *Biotechnol. Bioeng.* 2008, *100*, 839–854.

[7] Giovannini, R., Freitag, R., *Biotechnol. Bioeng.* 2001, *73*, 522–529.

[8] Schubert, S., Freitag, R., *J. Chromatogr. A* 2007, *1142*, 106–113.

[9] Schubert, S., Freitag, R., *J. Chromatogr. A* 2009, *1216*, 3831–3840.

[10] Bowles, M., Johnston, S., Schoof, D., Pentel, P., Pond, S., *Int. J. Immunopharmacol.* 1988, *10*, 537–545.

[11] Yazaki, P., Shively, L., Clark, C., Cheung, C-W., Le, W., Szpikowska, B., Shively, J., Raubitschek, A., Wu, A., *J. Immunol. Methods* 2001, *253*, 195–208.

[12] Gagnon, P., Cheung, C-W., Yazaki, P., *J. Immunol. Methods* 2009, *342*, 115–118.

[13] Ogawa, T., Hiraide, T., *Am. Lab.* 1996, *28*, 31–34.

[14] Bernardi, G., *Met. Enzymol.* 1973, *27*, 471–479.

[15] Kawasaki, T., Takahashi, S., Ikeda, K., *Eur. J. Biochem.* 1985, *152*, 361–371.

[16] Kawasaki, T., *J. Chromatogr.* 1991, *544*, 147–184.

[17] Gorbunoff, M., *Anal. Biochem.* 1984, *136*, 425–432.

[18] Gorbunoff, M., *Anal. Biochem.* 1984, *136*, 433–439.

[19] Gorbunoff, M., Timasheff, S., *Anal. Biochem.* 1984, *136*, 440–445.

[20] Luo, Q., Andrade, J., *J. Colloid Interface Sci.* 1998, *200*, 104–113.

[21] Bio-Rad Laboratories, CHT Ceramic Hydroxyapatite Instruction Manual, 2007 LIT611 Rev E.

[22] Gagnon, P., Ng, P., *Bioprocess Intnl.* 2005, *3*, 52–54.

[23] Harding, I., Rashid, N., Hing, K., *Biomaterials* 2005, *26*, 6818–6826.

[24] Ng, P., He, J., Gagnon, P., *J. Chromatogr. A* 2007, *1142*, 13–28.

[25] Hjerten, S., *Biochim. Biophys. Acta* 1959, *31*, 216–235.

[26] Diesenhofer, J., *Biochemistry* 1981, *20*, 2361–2370.

[27] Burton, D., *Mol. Immunol.* 1985, *22*, 161–206.

[28] Kabat, E., Tai, W., Perry, H., Gottesman, K., Foeller, C., Sequences of proteins of immunological interest, U.S. Dept. of Health and Human Services, Public Health Service, National Institute of Health, 1987.

[29] Bigelow, C., Channon, M., *Handbook of Biochemistry and Molecular Biology*, 3rd Edn., Proteins, Vol. 1, p. 209, CRC Press, Boca Raton, 1976.

[30] Fausnaugh-Pollitt, J., Thevenon, G., Janis, L., Regnier, F., *J. Chromatogr.* 1988, *443*, 221–228.

[31] Chicz, R., Regnier, F., *J. Chromatogr.* 1990, *500*, 503–518.

[32] Dismer, F., Hubbuch, J., *J. Chromatogr. A* 2007, *1149*, 312–320.

[33] Dismer, F., Petzold, M., Hubbuch, J., *J. Chromatogr. A* 2008, *1194*, 11–21.

[34] Yamamoto, S., Ishihara, T., *Sep. Sci. Technol.* 2000, *35*, 1707–1717.

[35] Sun, S., Removal of high molecular weight aggregates from an antibody preparation using ceramic hydroxyapatite chromatography, Oral presentation, *3rd International Hydroxyapatite Conference*, Lisbon, November 3–5, 2003.

[36] Sun, S., Ceramic hydroxyapatite chromatography in antibody and Fc-fusion protein purification. Oral presentation. *12th Annual Waterside Conference*, San Juan, Puerto Rico, April 23–25, 2007.

[37] Beam, K., Wu, H., Tsai, P., Evaluation of ceramic hydroxyapatite for removal of a 50 kDa mAb fragment and process-related impurities, Oral presentation *4th International Symposium on Hydroxyapatite*, Sonoma, May 4–6, 2008.

[38] Ng, P., Cohen, A., Gagnon, P., *Gen. Eng. News* 2006, *26*, 14.

[39] Freitag, R., Vogt, S., *Cytotechnology* 1999, *30*, 159–168.

